Desalination and Water Treatment
www.deswater.com

doi: 10.5004/dwt.2023.29164

284 (2023) 116–133
February

Nitrate removal from aqueous solutions using nanostructured adsorbents in continuous and discontinuous systems

Neda Baboli[a], Ali Bafkar[b,*]

[a]*Water Engineering Department, Faculty of Agricultural Science and Engineering, Razi University, Kermanshah, Iran, Mobile No.: 09182793701; email: neda3701@gmail.com*
[b]*Water Engineering Depatment, Razi University, Kermanshah, Iran, Mobile No.: 09183364231; Fax: 08338321083; email: alibafkar@yahoo.com*

Received 30 April 2022; Accepted 27 November 2022

ABSTRACT

Nitrate is one of the leading pollutants in water sources. The limitation of water resources and the increase of surface and underground water pollution by nitrate ions make it necessary to find acceptable environmental solutions to remove this substance from water sources. For practical applications, the adsorbent should have a high capacity, be cheap and easy to use. This research investigated the effect of eggshell, rice husk, wheat straw, and oak leaf nanostructured adsorbents on the removal of nitrate ions from aqueous solution by continuous and discontinuous systems. Discontinuous experiments studied the effect of factors such as pH, equilibrium time, optimal adsorbent mass and initial concentration of nitrate ions. Continuous experiments evaluated the effect of changes in the concentration of nitrate entering the column in increasing the efficiency of the adsorption column, and investigated the application of continuous models of adsorption in the description of breakthrough curves. According to the obtained results, the optimal pH of adsorption for the adsorbents under study was 5. Equilibrium time for eggshell, rice husk, and wheat straw nanostructured adsorbents was 30 and 120 min for oak leaf nanostructured adsorbents. By increasing the adsorbent mass from 0.3 to 1.6 g at the equilibrium time and optimal pH, the efficiency of nitrate ion adsorption has reached its peak by the nanostructured adsorbents of eggshell, rice husk, straw and wheat straw in the mass of 0.5 g and the oak leaf reached nanostructured adsorbent in the mass of 0.7 g. By increasing the initial concentration of nitrate ions from 5 to 120 mg/L, the efficiency of nitrate ion removal by eggshell, rice husk, wheat straw and oak leaf nanostructured adsorbents has decreased. The adsorption process was followed by Hove's kinetic model and Langmuir isotherm. The results of continuous tests showed that the total amount of nitrate absorbed and the adsorption capacity of the column increased with the increase of the concentration of nitrate entering the column, and the Thomas model was more consistent with the laboratory data. It is generally concluded that the eggshell, rice husk, wheat straw and oak leaf nanostructured adsorbents have the potential to remove nitrate ions.

Keywords: Nitrate; Nanostructured adsorbent; Equilibrium time; Optimal mass; Aqueous solution; Breakthrough curve

1. Introduction

Both in developed and industrialized countries, human activities play the biggest role in aggravating water shortage by polluting natural water sources. Drinking water contains large amounts of nitrate ions, which are a detriment to human health [1]. Contamination of water sources with nitrates has become an environmental problem across the

* Corresponding author.

globe. An increase in nitrate concentration in water sources causes methemoglobinemia in infants, diabetes in children, gastrointestinal cancers and abortion [2]. Nitrate contamination of surface and underground water mainly result from septic systems, agricultural runoff, animal waste and industrial processes. With the indiscriminate use of chemicals in the production process of agricultural products, the concentration of substances will exceed the maximum allowed concentration in soil, water, air and food products. This is not only fatal for humans, but it also causes the overall destruction of the environment by reducing biological power, imbalance in chemical balances and deep penetration of pollutants into underground water resources. Nowadays, it is necessary and inevitable to use different methods to purify or remove pollution from water and soil sources. Nitrogen as a nutrient (fertilizer) is widely used in pastures, gardens and fields. Different forms of nitrogen in the soil are converted into nitrate ions by bacteria. Nitrate easily penetrates into the ground by the passage of water through the soil layers, and due to heavy rain or irrigation, it reaches the roots of plants and finally the underground water. According to the standard of the World Health Organization, the maximum allowable concentration of nitrate in drinking water is 50 mg/L, while the United States Environmental Protection Agency (USEPA) has determined the maximum allowable concentration of nitrate in terms of nitrogen 10 mg/L, which is equivalent to 44.28 mg/L [3]. Various methods such as oxidation, reduction, precipitation, reverse osmosis, ion exchange and adsorption are used to remove nitrate, the most prominent of which is the surface adsorption process [4]. Various adsorbents have been used to remove nitrate from water [5]. The use of cheap adsorbents is one of the suitable methods to remove the pollutants in water [6]. Many studies have been already conducted on pollutant removal using cheap agricultural waste, including sawdust, Cedar tree [7], coconut shell powder [8] and lentil and wheat husk [9]. Agricultural residues, fruits and vegetable peels are the discarded waste materials and find no application anywhere. They can be used as low cost adsorbent after little processing. Agricultural wastes are mainly composed of lignin and cellulose and act as attractive alternative adsorbents due to their specific structure and chemical properties [10]. Nitrate removal was previously done by different adsorbents in microstructure dimensions, but nanotechnology has been recently used as a new technology to reduce water pollution. The advantages of using nanomaterials include self-constructing, increasing the contact surface with the adsorbent and high reactivity [11]. The use of nanomaterials and the manufacture of products in nanoscales has been growing in the last decade and it is expected to have an ascending trend in the future. Recently, nanomaterials are used in medical devices, drugs, agriculture, environmental cleaning, military and electronic applications [12]. Currently, metal nanoparticles are widely used in industrial products due to their unique properties. Therefore, nanotechnology is potentially used for water purification [13]. According to the above-mentioned, current study examined the effect of nano-adsorbents of eggshell, rice husk, wheat straw and oak leaf on nitrate adsorption in discontinuous and continuous systems. Discontinuous experiments studied the effect of factors such as pH, equilibrium time, optimal adsorbent mass and initial concentration of nitrate ions. Continuous experiments evaluated the effect of changes in nitrate concentration entering the column in increasing the efficiency of the adsorption column.

2. Materials and methods

2.1. Preparation of studied adsorbents

Eggshell, rice husk, wheat straw and oak leaf adsorbents were prepared for this research. Upon their transfer to the laboratory, the prepared adsorbents were washed several times with distilled water and dried in the open air [14]. Then, the dried adsorbents were ground due to their coarseness to turn them into smaller nanometer particles. To prepare adsorbents in the nanostructure scale, the dried adsorbents were put into a ball mill until being converted into nanometer dimensions [15]. The preparation of the nanostructure of the adsorbents was done in 3 h and with a frequency (the number of swings and turns of the moving lever of the mill per second) of 28 (1 s). After the mentioned time, in order to check the diameter of nanoparticles, granulation analysis was performed on the particles. The ball mill used in this research had two steel cylinders with an agate inner wall of 35 mL volume, and an agate ball is placed in each of these cylinders. The cylinders must be mounted on the moving levers of the device and the movement of these levers can be adjusted at different frequencies. Cylinders oscillate horizontally around their axis. RETSCH-MM200 model ball mill was used in this study.

2.2. Characteristics of the studied adsorbents

Adsorbent characterization tests were performed including particle size classification (PSA) [16], the apparent morphology of the adsorbent surface using a scanning electron microscope [17], the quantitative analysis system of the elements in the adsorbent [18] energy-dispersive X-ray analysis (EDAX) and also the determination of functional groups in the adsorbent Fourier-transform infrared spectroscopy (FTIR) [19].

2.3. Preparation of nitrate solution

The initial solution (mother solution) with a concentration of 1,000 mg/L was obtained by dissolving 1.63 g of potassium nitrate salt in 1 L of deionized water. Mother solution and deionized water were used to make a solution with other required concentrations. To perform the experiments, 650 mL Falcons (for each concentration) were washed with distilled water. Nitrate adsorption from the equilibrium solution using the studied nano-adsorbents were investigated under the following conditions: pH 3, 4, 5, 6, 7 and 8, contact time 10, 30, 60, 90, 120 and 180 min, adsorbent mass 0.3, 0.5, 0.7, 1, 1.3 and 1.6 g, initial concentration of nitrate 5, 10, 30, 60, 90 and 120 mg/L. After the mentioned times, the adsorbents were separated from the liquid phase using a centrifuge at a speed of 2,000 rpm and a duration of 15 min, then the samples were passed through ribbed filter paper and finally the concentration

of remained nitrate was measured using a spectrophotometer model (EL02095801, UV-Visible) with a wavelength of 600 nm. Nitrate adsorption percentage and adsorption capacity of adsorbents were determined from Eqs. (1) and (2), respectively [20].

$$\%R = \frac{C_i - C_f}{C_i} \times 100 \tag{1}$$

$$q = \frac{C_i - C_f}{m} \times V \tag{2}$$

where q was the amount of adsorption of the dissolved substance per unit mass of the adsorbent (mg/g); C_i, initial concentration of the solute (mg/g); C_f, the remaining concentration of the solute (mg/g) after the equilibration time has passed; m the amount of adsorbent (g) and V was the volume of the solution (L).

2.4. Adsorption kinetics test

Non-equilibrium or kinetic equations are those that are used before creating equilibrium and the time plays a major role in them. In this case, changes in absorbed substance (q_t) with time are shown [21]. Adsorption kinetic tests were performed by solutions containing nitrate with concentrations of 5, 10, 30, 60, 90 and 120 mg/L, optimal acidity and optimal adsorbent amount. The test solutions were placed on the stirrer for 30 min at a speed of 120 rpm. As the above times passed and the adsorbent was separated from the solution, the amount of nitrate solution was read. Finally, the kinetic models in Eq. (3) [22] and Eq. (4) [23] were fitted to the test data and their coefficients were calculated.

$$q_t = q_e\left(1 - \exp\left(-k_1 t\right)\right) \tag{3}$$

$$q_t = \frac{k_2 q_e^2 t}{1 + q_e k_2 t} \tag{4}$$

where q_e is the equilibrium adsorption capacity (mg/g); q_t, amount of adsorbed ion at time t (mg/g); K_1 Lagergren adsorption constant (min^{-1}); K_2 the constant of Ho and McKay equation (g/mg·min).

2.5. Adsorption isotherm test

Equilibrium equations or adsorption isotherms are equations that show the distribution of the adsorbed substance between the dissolved and adsorbed phase in the equilibrium state and are considered a characteristic for the system at a certain temperature. Two parameters q_e and C_e are used to describe the equilibrium state, where q_e is the amount of substance adsorbed per unit weight of the adsorbent and C_e is the concentration of the remaining component in the solution [24]. The adsorption isotherm was performed by solutions containing nitrate with an initial concentration of 10 mg/L, optimal acidity and optimal amount of adsorbent. The solutions were placed on the shaker at a rate of 120 rpm. At the time of equilibrium, the samples were removed from the shaker and after separating the adsorbents, the amount of nitrate remaining in the solution was read and finally the isotherm models in Eq. (5) [25] and Eq. (6) [26] were fitted on the test data and their coefficients were calculated.

$$q_e = \frac{x}{m} = \frac{bq_m C_e}{\left(1 + bC_e\right)} \tag{5}$$

$$q_e = \frac{x}{m} = kC_e^{1/n} \tag{6}$$

where q_e, equilibrium adsorption capacity (mg/g); x, the mass of material absorbed on the adsorbent (mg); m, mass of adsorbent used (g); b, Langmuir constant (L/mg); q_m, the maximum equilibrium adsorption capacity to complete a layer (mg/g), C_e, the concentration of adsorbed substance in the equilibrium state in the liquid phase (mg/L), and n and k are Freundlich model coefficients.

2.6. Continuous tests

A glass column with a fixed bed (inner diameter 4.3 cm and height 84 cm) and an inlet flow rate of 50 mL/min was used for the tests. According to Fig. 1, at the bottom of the adsorption bed, a glass filter with a pore diameter of 400 μ was placed to prevent the exit of fine particles of the adsorbents. Also, fiber glass was used to evenly distribute the solution entering the column on the entire surface of the adsorbents. The adsorbents used in the continuous tests have an approximate size of 500 μ, and to reach this size, sieve No. 20 (with a pore diameter of 841 μ) and 40 (with a pore diameter of 420 μ) were used. Nitrate solution with a pH of 5 and concentrations of 5, 10 and 30 mg/L was fed to the peristaltic system at laboratory temperature (22°C) as a gravity flow using a pump [27].

The efficiency of an adsorption column is described by the breakthrough curve, which indicates the behavior of the adsorbent (nitrate) during removal from the solution containing it along the length of the column bed, and it is generally defined in the form of normalized concentration as the ratio of output to input concentration per unit time or the output volume for a specific bed [Eq. (7)] [28].

$$V_{\text{eff}} = Qt \tag{7}$$

where Q and t are volume flow in mL/min and total flow time in min, respectively.

The area under the breakthrough curve (A) can be calculated by integrating the adsorbed nitrate concentration curve (C_{ad}) vs. time (t) and it can be used to calculate the total amount of adsorbed ions (q_{total}) in the column for the input concentration and the given flow rate [Eq. (8)] [29].

$$q_{\text{total}} = \frac{QA}{1000} = \frac{Q}{1000}\int_{t=o}^{t=\text{total}} C_{\text{ad}}\,dt \tag{8}$$

The total amount of ions entering the column (m_{total}) and total removal percentage can be calculated from Eqs. (9) and (10), respectively [30].

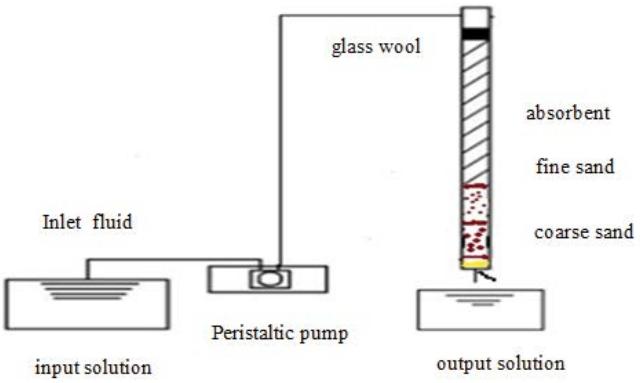

Fig. 1. Schematic image of the laboratory column used in continuous experiments.

$$m_{\text{total}} = \frac{C_0 Q t_{\text{total}}}{1{,}000} \tag{9}$$

$$\text{Total Removal}(\%) = \frac{q_{\text{total}}}{m_{\text{total}}} \times 100 \tag{10}$$

The adsorption capacity of the column (q_{eq}) can be calculated using Eq. (11) as the total amount of ions adsorbed at the end of the total flow time (q_{total}) per unit mass of the adsorbent X [31].

$$q_{\text{eq}} = \frac{q_{\text{total}}}{X} \tag{11}$$

The empty bed residence time (EBRT) represents the time required for the empty column to be filled by the solution in minutes, which can be calculated from Eq. (12) [32].

$$\text{EBRT} = \frac{\text{Bed Volume}}{\text{The flow rate of the input stream to the column}} \tag{12}$$

The volume of the bed is in mL and the flow rate of the input flow to the column is in mL/min.

2.7. Continuous adsorption models

2.7.1. Bohart–Adams model

The Bohart–Adams model is based on the surface reaction rate theory, and based on that, it is assumed that the equilibrium is not instantaneous. This model is usually chosen to describe the initial parts of the breakthrough curve of a fixed bed column [30]. The Bohart–Adams model is expressed in following equation:

$$\ln\left[\frac{C_t}{C_0}\right] = K_{\text{AB}} C_0 t - \frac{K_{\text{AB}} N_0 Z}{U_0} \tag{13}$$

where K_{AB} represents the Bohart–Adams kinetic constant (L/mg·min), N_0 and Z are the maximum volumetric adsorption capacity (mg/L) and the depth of the column bed (cm), respectively and U_0 is the linear velocity obtained from the result of dividing the inlet flow rate by the cross-sectional area of the column (cm/min) [33].

2.7.2. Thomas model

The Thomas model is widely used to investigate the performance of adsorption columns [34]. This model is obtained from the equation of conservation of mass in a flow system, which expresses how the adsorption rate obeys the reversible quadratic kinetic models. In addition, this model ignores both intraparticle and external mass transfer resistance. Therefore, the adsorption of the solute on the adsorbent takes place directly, which means that the adsorption rate is controlled by the surface reaction between the adsorbent and the empty capacity of the adsorbent [35]. The mathematical form of this model is as Eq. (14). where C_0 are the concentration of metal ions in the outlet and inlet flows respectively (mg/L). K_{Th} is Thomas speed constant (L/g·min), Q flow intensity (mL/min), q_0 maximum adsorption capacity (mg/g), M mass of dry adsorbent (g), t is time (min) [36].

$$\ln\left[\frac{C_0}{C_t} - 1\right] = \frac{K_{\text{Th}} q_0 m}{Q} - K_{\text{Th}} C_0 t \tag{14}$$

2.7.3. Yoon–Nelson model

Yoon–Nelson model was developed based on the adsorption theory and the probability of failure of the adsorbed material. This model is simple and includes fewer parameters and column data and can be used for a single component system [37]. This model is expressed as follows:

$$\ln\left[\frac{C_t}{C_0 - C_t}\right] = K_{\text{YN}} t - \tau K_{\text{YN}} \tag{15}$$

In the Yoon–Nelson model, K_{YN} and τ represent the Yoon–Nelson constant (min^{-1}) and the time required for 50% breakdown of the adsorbent material (min).

2.7.4. Evaluation criteria of models

The use of efficient and effective models to fit the data obtained from adsorption tests is one of the main parts of the studies related to the adsorption and treatment of wastewater. Therefore, the use of evaluation methods of these models is of particular importance. To evaluate the models used in this research, RMSE, R^2 criterion was used. However the RMSE value is lower, it means that the fitted values are closer to the true values. If the value of R^2 is close to 1, this indicates a high correlation between the fitted and obtained values [38].

$$\text{RMSE} = \sqrt{\frac{\sum_{i=1}^{n}\left(q_e - q_c\right)^2}{n}} \tag{16}$$

$$R^2 = \left[\frac{\sum_{i=1}^{N}\left(q_c - q_{\text{cm}}\right)\left(q_e - q_{\text{em}}\right)}{\sqrt{\sum_{i=1}^{N}\left(q_c - q_{\text{cm}}\right)^2}\sqrt{\sum_{i=1}^{N}\left(q_e - q_{\text{cm}}\right)^2}}\right] \tag{17}$$

where q_c is the value obtained from fitting the model; q_e, the value obtained from the test; q_{cm}, the average value obtained from the model fitting, q_{em}, the average value obtained from the test and n is the number of test components.

3. Results and discussion

3.1. Properties of studied adsorbents

The results of nanoparticle size analysis (PSA) of eggshell, rice husk, wheat straw and oak leaf adsorbents are shown in Fig. 2, respectively. According to Fig. 2A, 100% of eggshell adsorbent particles were in the range of nanostructure with a diameter less than 101.5, Fig. 2B., rice husk were in the range of nanostructure with a diameter less than 118.6, Fig. 2C, wheat straw in the range of nanostructure with a diameter less than 110 and Fig. 2D, oak leaf in the range of nanostructure with a diameter of less than 98.74 nm. As can be seen, the studied adsorbents were transformed into nanostructured particles.

3.2. Quantitative analysis results of elements present in the studied nanostructured adsorbents

Fig. 3 shows the results of the quantitative analysis of the studied adsorbents using EDAX analyzer. It is noteworthy that the gold displayed in the shapes is related to the gold coating that was placed on the samples.

According to Fig. 3A, the adsorbent structure of eggshell has calcium and copper.

According to Fig. 3B, the adsorbent structure of rice husk has silicon, potassium, copper and zinc.

According to Fig. 3C, the adsorbent structure of wheat straw has silicon, potassium, calcium, copper and zinc.

According to Fig. 3D, the adsorbent structure of oak leaf has silicon, potassium, calcium, copper and zinc.

3.3. Scanning electron microscopy test results

The results of measuring the morphology of eggshell, rice shell, wheat straw and oak leaf nanostructured adsorbents using scanning electron microscopy (SEM) analysis are shown in Fig. 4. According to the figure, it can be seen that there are deep dimples on the surface of the absorbers and it has a complex, tangled, uneven and irregular structure. By changing the size of the adsorbent particles to the size of the nanostructure, the specific surface area of the adsorbent is increased, so it is expected that the studied adsorbents have a high potential to adsorb ions [39].

3.4. FTIR test results

Fig. 5a–h are related to the IR spectrum of eggshell, rice husk, wheat straw, and oak leaf nanostructure adsorbents before and after adsorption. Bonded vibrational frequencies

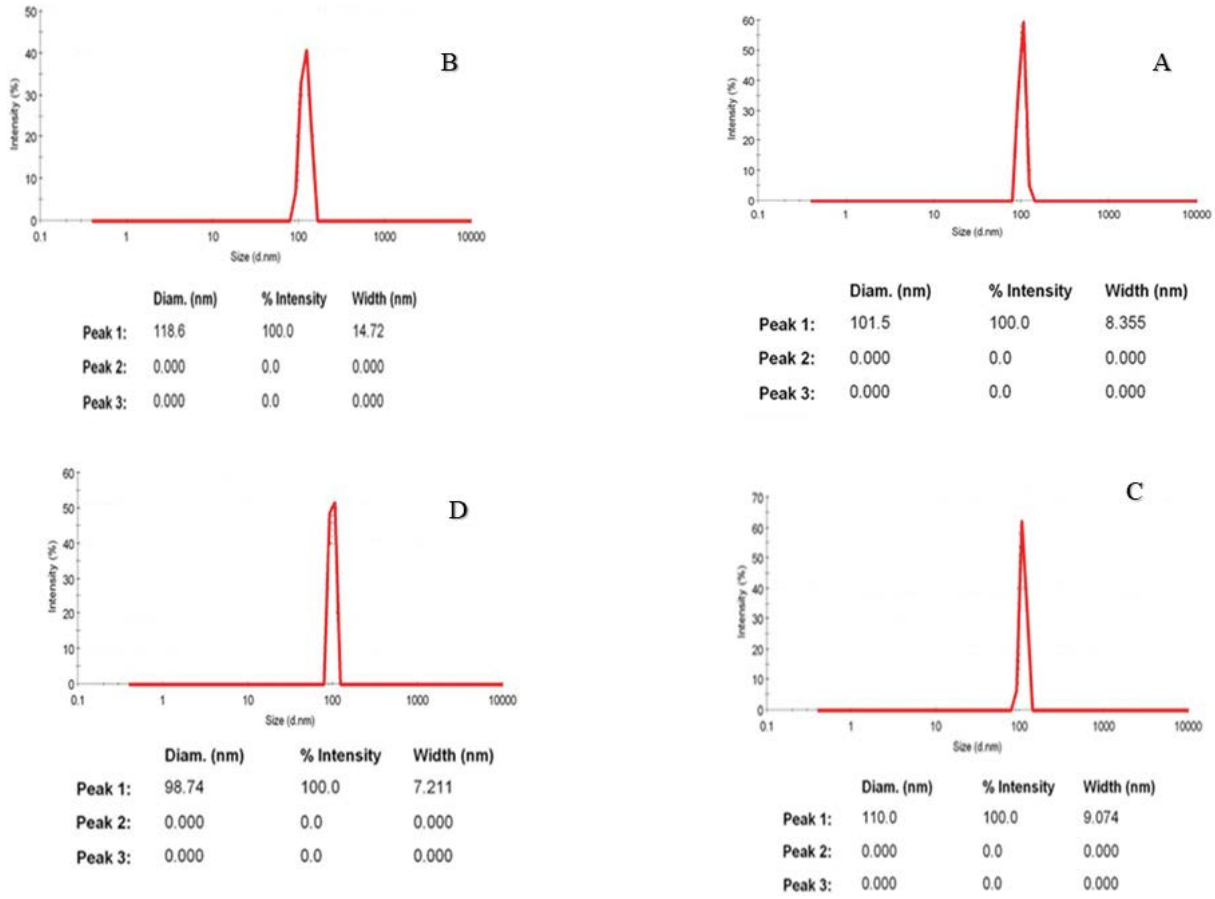

Fig. 2. Analysis of the studied nanosorbent particle granulation (PSA).

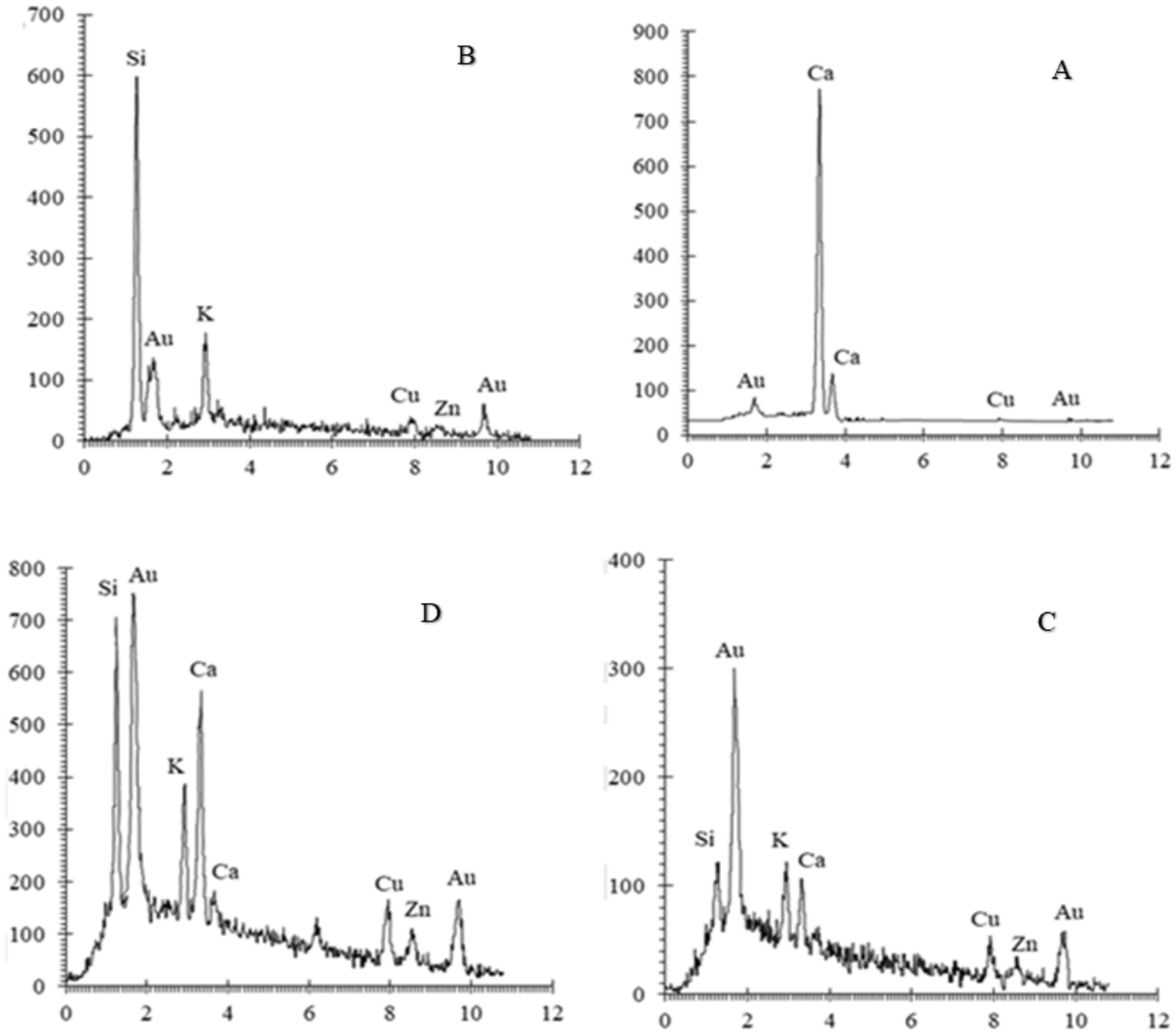

Fig. 3. Quantitative analysis results (EDAX) of the elements found in the studied sorbents.

are as follows: the wave frequency above 3,000 cm^{-1} corresponds to the average adsorption of the symmetric stretching vibrations of OH…OH hydrogen bonds, the wave frequency between 2,800–2,900 cm^{-1} corresponds to the stretching vibrations of the C–H bond (group of alkanes) and the wavelength between 1,600 and 1,700 cm^{-1} is related to the C=O bond and the adsorption peak above 1,040 cm^{-1} is related to the C–O bond (esters group) [40]. Also, comparison of nitrate removal by different nano-absorbent is shown in Table 1.

3.5. Effect of pH on nitrate adsorption

The pH of the solution is an important parameter in the study of the adsorption process. Adjusting the pH of ion-contaminated environments is very important, therefore it is necessary to examine the tests related to the effect of this parameter on the adsorption rate before any other tests [41]. The research shows that the optimum pH for nitrate adsorption is often in the range of 3–8. At low pH, hydrogen ions are considered as competitors in the environment and by sticking on the adsorbent surface, it reduces the adsorption sites on the adsorbent, also with the increase of pH, the reason for the increase in efficiency can be the high specific surface area of the adsorbent due to the fineness of the adsorbent and the increase in porosity and the increase in the number of functional groups in the adsorbent [42]. The results of the effect of different pH on nitrate adsorption by eggshell, rice husk, wheat straw and oak leaf are shown in Fig. 6. As can be seen in Fig. 6, at all pH levels, nitrate adsorption by eggshell is higher than other adsorbents. Maximum adsorption of nitrate by eggshell, rice husk, wheat straw and oak leaf is 98.03%, 92.51%, 89.15% and 94.22%, respectively. In this study, the removal efficiency of nitrate by eggshell, rice husk, wheat straw and oak leaf adsorbents was high

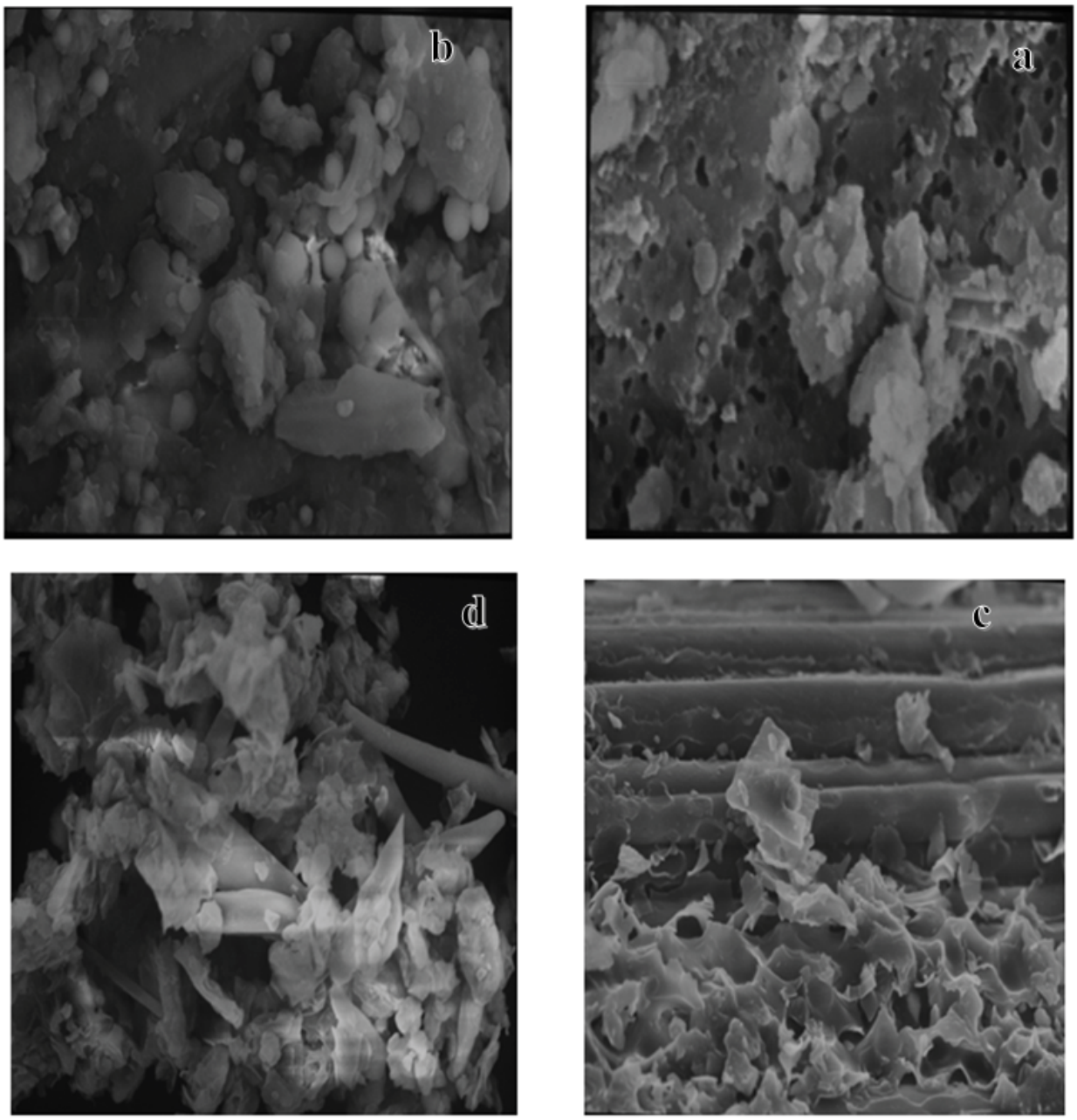

Fig. 4. SEM images of eggshell sorbent, (A) (magnification of 10,000), rice husk sorbent, (B) (magnification of 2,000), wheat straw sorbent, (C) (magnification of 1,000), and oak leaf sorbent (D) (magnification of 1,000).

at pH = 5 and the removal efficiency decreased as pH increased.

3.6. Effect of time on nitrate adsorption

The results of determining the optimal time of nitrate adsorption at optimal pH for all four adsorbents are shown in Fig. 7. In the early times, the rate of nitrate adsorption by eggshell, rice husk, wheat straw, and oak leaf adsorbents was very high, and as contact time increased, the adsorption efficiency increased and then after some decrease, it remained almost constant. The maximum amount of nitrate adsorption by eggshell, rice husk, and wheat straw was obtained at 30 min of contact time, and the maximum amount of nitrate adsorption by oak leaf was obtained at 120 min of contact time.

3.7. Effect of adsorbent amount on nitrate adsorption

The results of determining the amount of nitrate adsorption for all four adsorbents are shown in Fig. 8. Increasing the amount of eggshells, rice husks, wheat straw and oak leaf initially increased nitrate adsorption. Increasing the amount of eggshells, rice husks and wheat straw to more than 0.5 g and increasing the amount of oak leaf to more

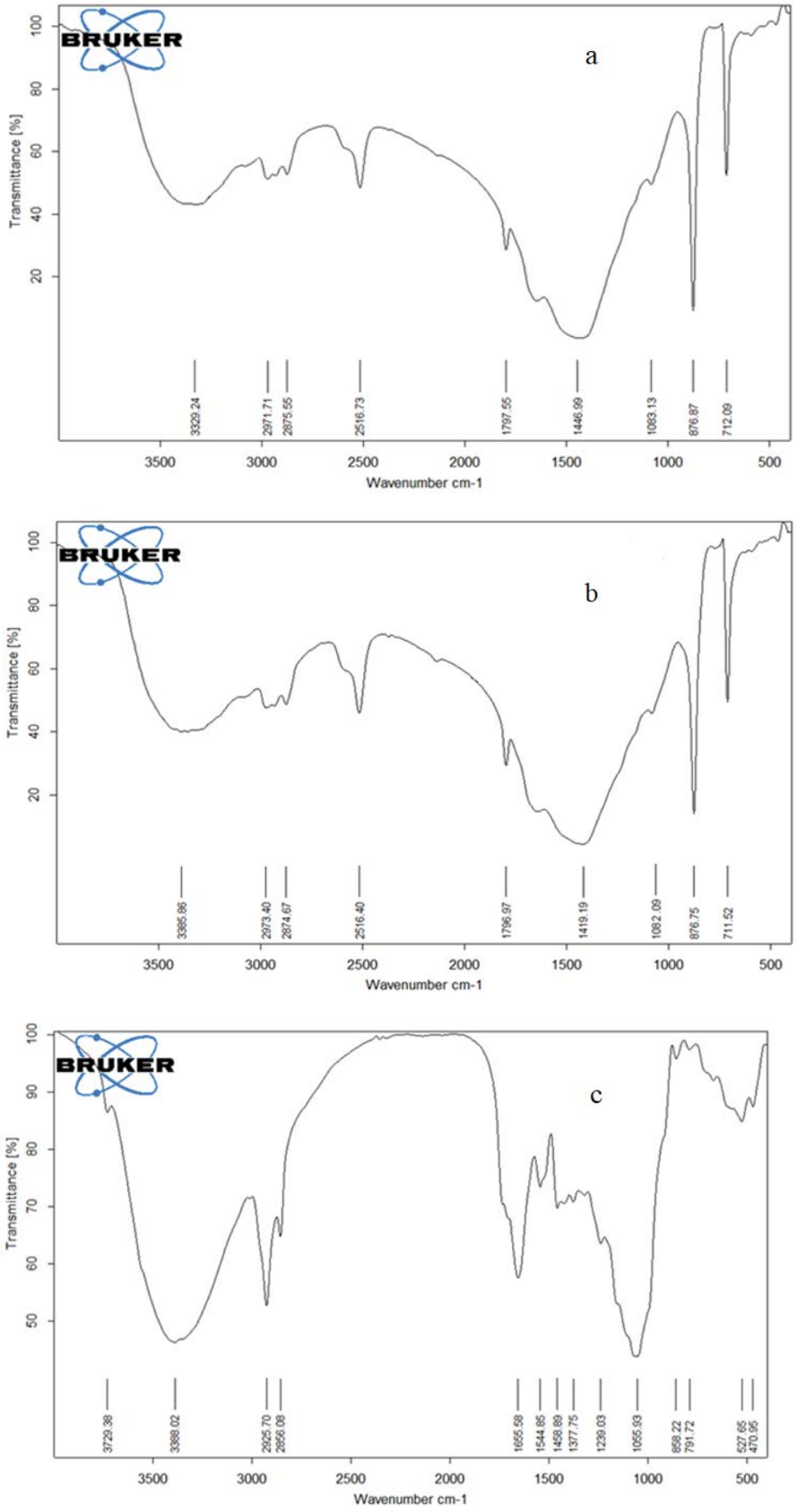

(Fig. 5. Continued)

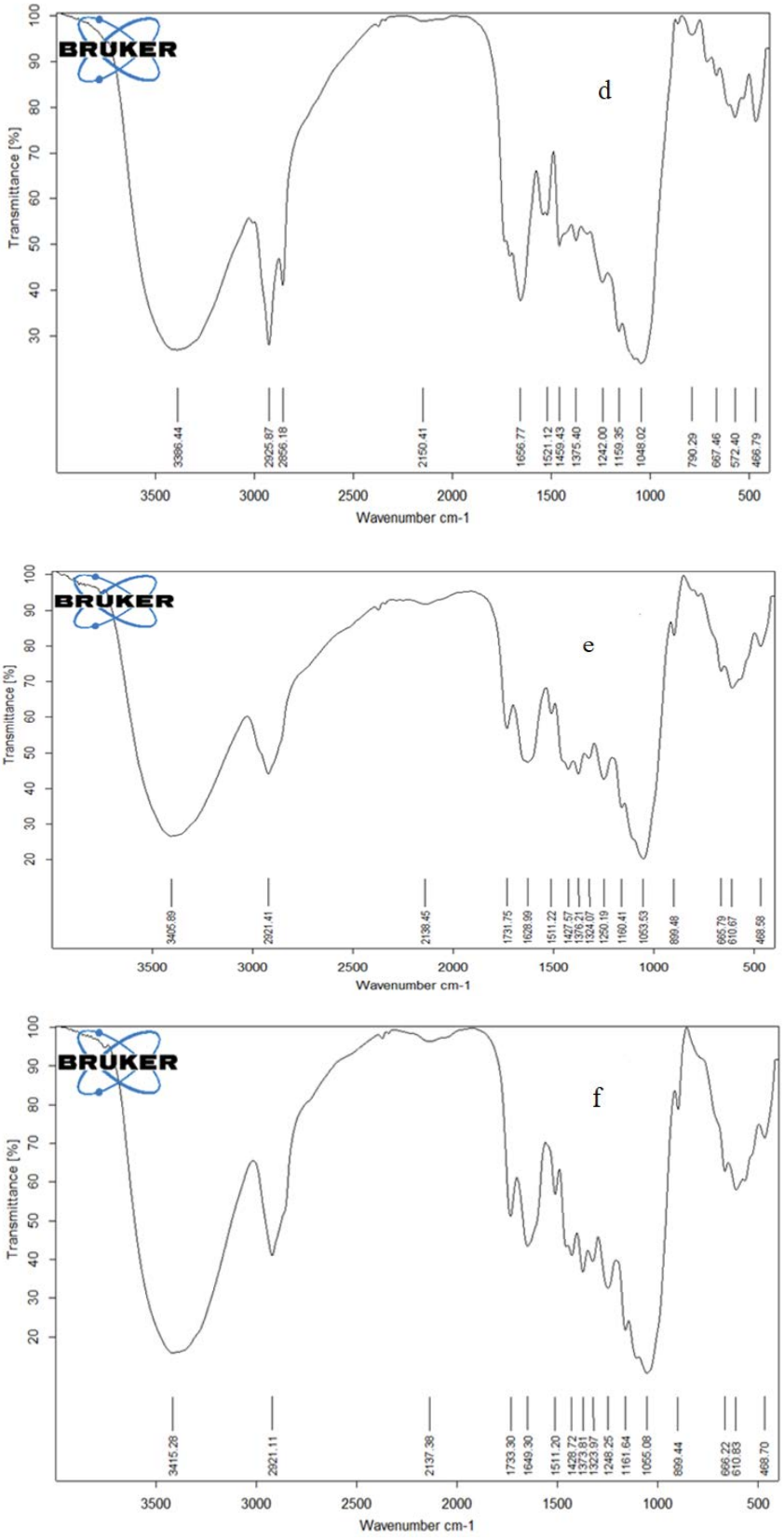

(Fig. 5. Continued)

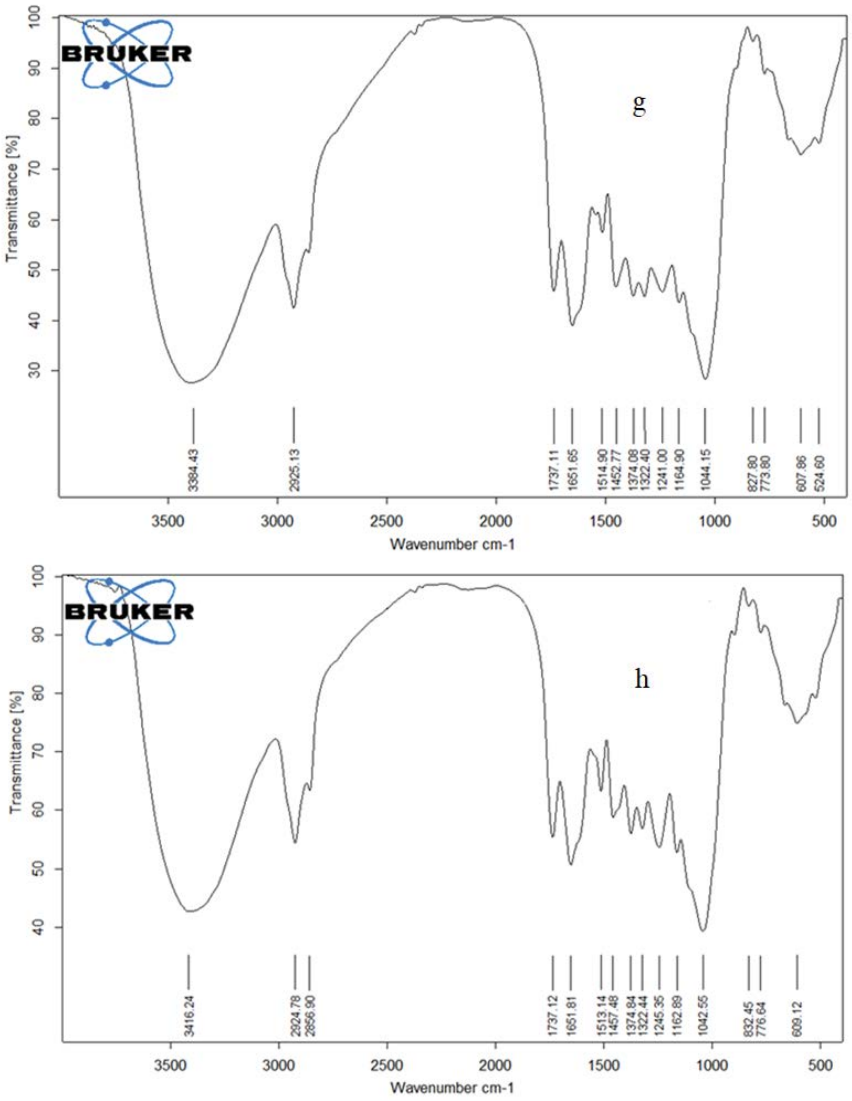

Fig. 5. Fourier-transform infrared (FTIR) graph before and after adsorption of nitrate ions.

Table 1
Comparison of nitrate removal by different nano-absorbent

S. No.	Adsorbent	Adsorbate	pH	Contact time	Dosage	Initial concentration	References
1	Modified wheat straw	Nitrate	7	10 min	2 g/L	20 mg/L	[44]
2	Activated carbon	Phosphate and nitrate	6	30 min	–	–	[45]
3	Ammonium-functionalized magnetic mesoporous silica	Nitrate	6	60 min	0.2 g/L	300 mg/L	[46]
4	*Pseudomonas mendocina* GL6 immobilized on biochar	Nitrate	7	–	–	100 mg/L	[57]
5	Carbon/silicon	Nitrate	–	60 min	0.1 g/L	50 mg/L	[47]
6	Local clay	Nitrate	2	120 min	4 g/L	100 mg/L	[48]

than 0.7 g had no effect on the adsorption efficiency of nitrate. The maximum efficiency of nitrate adsorption by eggshell, oak leaf, rice husk, and wheat straw adsorbents is 97.24%, 93.82%, 93.50%, and 90.14%, respectively.

3.8. Effect of initial concentration on nitrate adsorption

The effect of initial concentration of nitrate with changing solution concentrations (5, 10, 30, 60, 90 and 120 mg/L) for all four adsorbents is shown in Fig. 9. As can be seen, with the increase in the concentration of the solution, the adsorption efficiency has decreased for all adsorbents [43]. The maximum efficiency of nitrate adsorption by eggshell, oak leaf, rice husk, and wheat straw adsorbent was obtained as 99.42%, 94.41%, 92.54% and 89.49%, respectively.

3.9. Adsorption kinetics test

Adsorption kinetics is studied to better understand the adsorption dynamics of desired ions on the adsorbent surface. According to Table 2, the highest RMSE for eggshell, rice husk, wheat straw and oak leaf adsorbents (8.07, 8.39, 7.82 and 4.85, respectively) was related to the Lagergren model. Hove's model for the desired adsorbents with higher R^2 (0.89, 0.89, 0.89 and 0.99 respectively) and lower RMSE (0.74, 0.78, 0.73 and 0.15, respectively) had the most compliance with the adsorption data. According to the adsorption capacity calculated by Hove and Lagergren's model, the adsorption capacity predicted by Ho model was more consistent with the laboratory adsorption data than that of Lagergren's model [49].

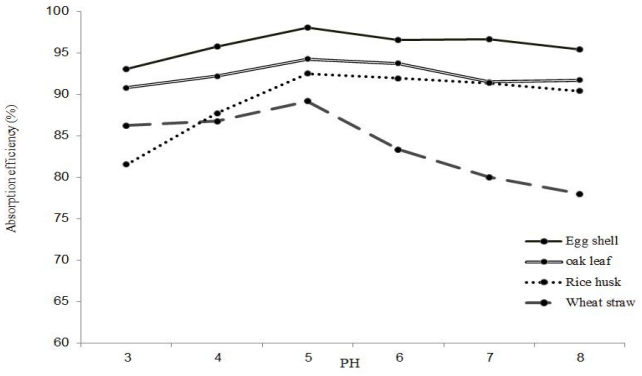

Fig. 6. Changes in nitrate adsorption efficiency with pH for the studied adsorbents.

3.10. Adsorption isotherm test

Examining isotherms is an important parameter in adsorption studies. The isotherm studies of nitrate ion adsorption by eggshell, rice husk, wheat straw, and oak leaf adsorbents are shown in Table 3. According to the obtained correlation coefficient values, it was observed that the Freundlich two-parameter model had a higher R^2 and a lower RMSE than the Langmuir model. Similar results were obtained by Karthikeyan et al. [50].

3.11. Results of continuous tests

In order to create the optimal performance of the continuous flow column, the initial concentration of nitrate input was changed in the range of 5, 10, and 30 mg/L. The effect of the inlet concentration of adsorbent at a bed height of 40 cm and a flow rate of 50 mL/min by the breakthrough curve for eggshell (a), rice husk (b), and wheat straw (c) and oak leaf (d) adsorbents are shown in Fig. 10, respectively. According to the figure, it can be seen that with the increase of the input concentration from 5 to 30 mg/L, the volume of the adsorbed material that enters the column increases and causes more adsorption of ions on the adsorption sites and it is broken as a result of the early adsorbent saturation and the time reduction [51].

Table 4 shows that for the adsorbents under study, the highest adsorption rate and maximum nitrate adsorption capacity were obtained at the highest ion concentration (30 mg/L). According to the results, it was observed that with the increase in the input nitrate concentration, the adsorption capacity increased, which was probably caused by the gradient of the concentration and the driving force that increased the adsorption process, but all the adsorption

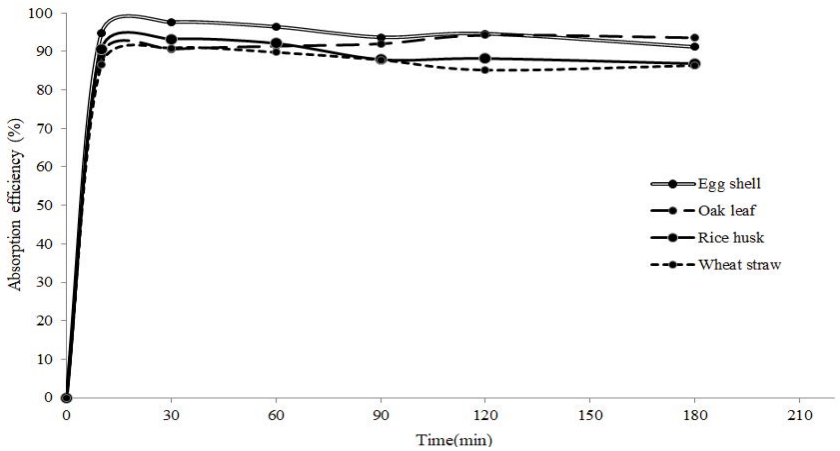

Fig. 7. Changes in nitrate adsorption efficiency with time for the studied adsorbents.

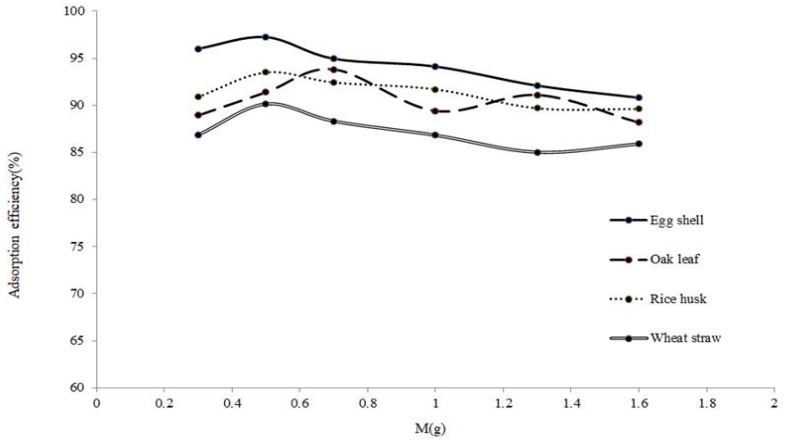

Fig. 8. Nitrate adsorption efficiency in different amounts of studied adsorbents.

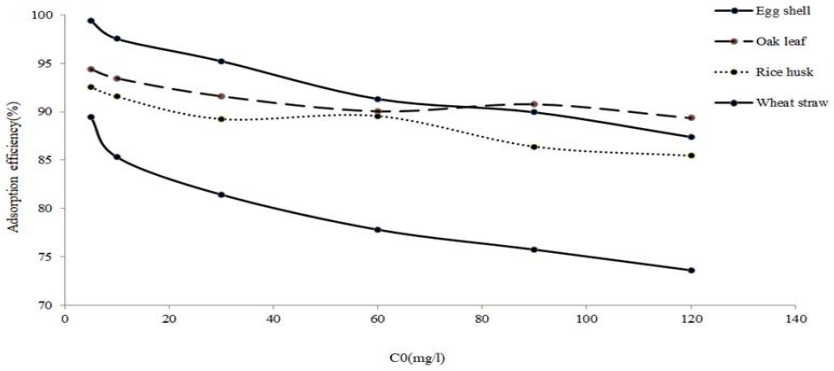

Fig. 9. Effect of initial concentration of nitrate on the adsorption efficiency of the studied adsorbents.

sites were quickly filled, so the total percentage of removed nitrates decreased.

3.12. Fitting continuous adsorption models

In this part of the study, the dynamic behavior of nitrate adsorption by eggshell, rice husk, wheat straw, and oak leaf adsorbents was investigated using Adams–Bohart, Thomas and Yoon–Nelson models. The parameters predicted by these models in nitrate adsorption by eggshell, rice husk, wheat straw, and oak leaf in different concentrations are shown in Table 5. According to the table, in fitting the Adams–Bohart model, with the increase in the initial concentration, there is an increase in the values of N_0 (maximum volumetric adsorption capacity), and this increase in concentration increases the ion input to the column and the faster saturation of the adsorbent in it, and finally, reduces the breakthrough time [52]. In fitting the Thomas model, with the increase in the initial concentration, it was observed that the values of the maximum adsorption capacity (q_0) increased and the constant of the Thomas velocity (K_{Th}) decreased, which might be due to the fact that with the increase of the input concentration, the loading rate of the pollutant with the bed increased and the thrust force to transfer the mass increased and while the length of the mass transfer area is shortened, the bed breakthrough has occurred in a shorter time. At higher initial concentrations, the available adsorption sites are more limited and this has decreased the ion adsorption rate or the Thomas rate constant [53]. In the Yoon–Nelson model as seen in Table 5, the K_{YN} increases with increasing flow while τ decreases due to decreasing contact time [54].

4. Discussion

In acidic pH, the surface of adsorbents increases due to the presence of H^+ ions and the electrostatic force between the surface of adsorbents and nitrate ions [55]. In a research by Karthikeyan et al. [56] to remove nitrate and phosphate using amine crosslinked magnetic banana bract activated carbon, the range of pH 2 to 12 was investigated. In this study, the highest amount of nitrate removal occurred at pH = 7, and after that, the adsorption efficiency followed a decreasing trend [56]. Also, in a study by Zhang et al. [57], the highest nitrate removal efficiency was obtained using *Pseudomonas mendocina* GL6 immobilized on biochar at pH = 8. At the beginning of the test, the empty places of the adsorbents are very high, and with the passage of time due to the decrease of the empty places, the amount of nitrate adsorption decreased [58]. Farasati et al. [59] obtained the equilibrium time for nitrate removal by micrometer *Phragmites australis* anion exchange as 180 min. Kumar et al.

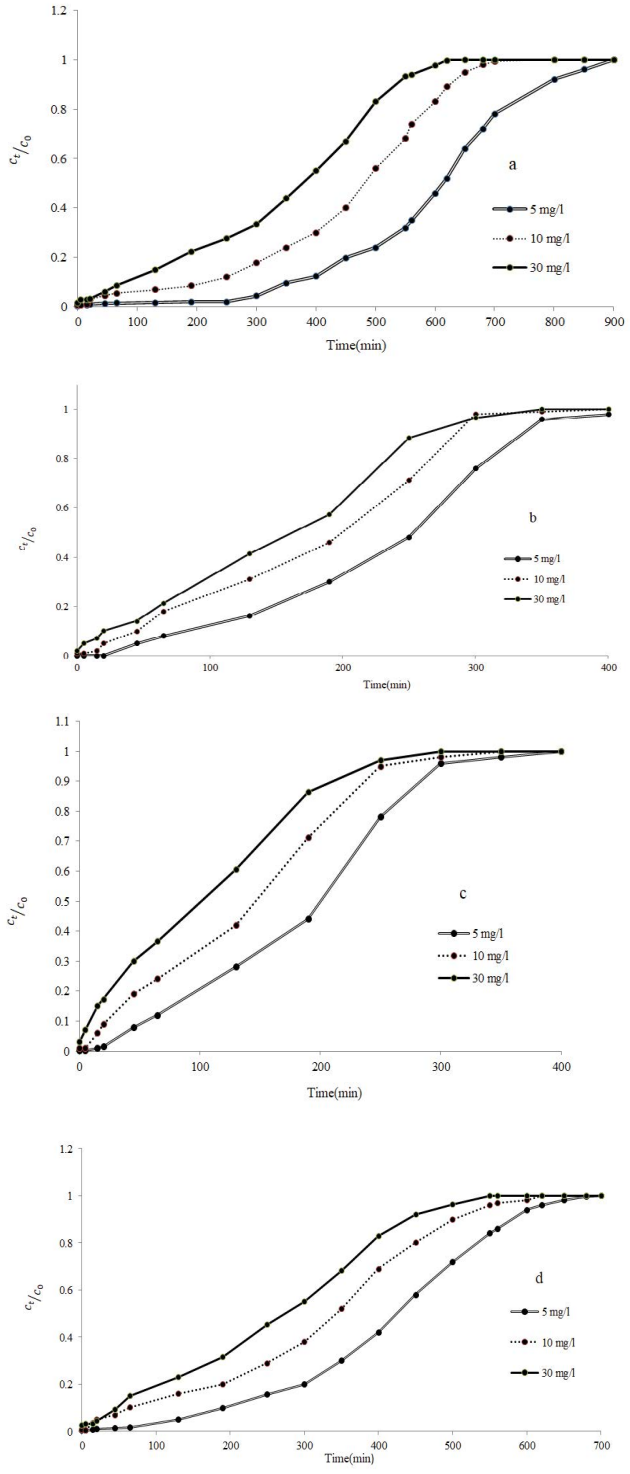

Fig. 10. Fragility curve of nitrate removal by sorbents in different concentrations (flow rate 50 mL/min).

[60] calculated the equilibrium time for nitrate removal using polyvalent metal ions to be 40 min. In addition, with the increase in the amount of adsorbent, the efficiency of nitrate ion adsorption first increased and then no significant increase was observed and the adsorption capacity decreased. This phenomenon can be justified by the fact that nitrate adsorption by all four adsorbents due to the increase in Eigen level and adsorption sites initially increased [61]. But when the adsorption process was complete, adding more adsorbent did not affect it [62]. Alimohammadi et al. [14] obtained the optimal amount of magnetic multi-walled carbon adsorbent for nitrate adsorption equivalent to 5 g/L, and also Takdastan et al. [69] obtained the optimal amount of activated carbon adsorbent for removing nitrate equivalent to 5 g/L. In addition, Rahdar et al. calculated the optimal amount of copper oxide adsorbent for nitrate adsorption equal to 0.08 g/L [63]. At low concentration, the Eigen level and adsorption sites of the adsorbents were high, and nitrate ions have interacted with the functional groups on the surface of the adsorbent and the adsorption efficiency has increased. At higher concentrations, adsorption efficiency has reduced due to the saturation of the adsorption sites [64]. Wang et al. obtained the highest nitrate adsorption by green tea and eucalyptus leaf extracts at a concentration of 20 mg/L [65]. Also, Fotsing et al. [66] obtained the highest nitrate adsorption efficiency by amine-modified cocoa shell at a concentration of 300 mg/L. Also, in continuous experiments, with the increase of the input concentration, the slope of the breakthrough curve increases and the volume of breakthrough decreases due to the reduction of the mass transfer load between the solution and the surface of the adsorbents and the reduction of the driving force. This is because, in the low nitrate concentration, reduction of the mass transfer driving force and diffusion coefficient led to better diffusion of nitrate towards the adsorbent pores; consequently, the contact time increased and the solution left the column later. Hence, the adsorption ability of the adsorbents increased in lower concentrations. However, in the greater inlet concentrations, the breakthrough times moved to the origin and left. This is because, with increasing concentration, the driving force was increased for diffusion of nitrate in the column [67]. Azari et al. [68] investigated the removal of nitrate from water environments by carbon nanotubes magnetized with iron nanoparticles. In this study, the pH equal to 3, 60 min contact time, 200 rpm stirring speed and 1 g/L absorbent was obtained as the optimum conditions in the adsorption of nitrate. Investigating the isotherm and kinetic models showed that the experimental data correlate to the Langmuir adsorption isotherm model ($R^2 > 0.997$) and pseudo-second-order kinetic ($R^2 > 0.993$). Takdastan et al. [69] investigated the efficiency of activated carbon nanocomposite@Fe_3O_4 and ultrasonic waves (US) in removing nitrate from aqueous solution. This study examined the effects of different parameters on nitrate removal including contact time, pH, nanocomposite dose, initial nitrate concentration and temperature. Equilibrium adsorption data were analyzed using four common adsorption models. In addition, kinetic and thermodynamic parameters were used to establish the adsorption mechanism. The results of this research indicated high removal efficiency at pH 3, equilibrium time 90 min and adsorbent dosage 2 g/L. Nitrate removal also followed the Langmuir isotherm with $R^2 = 0.996$ and pseudo-second-order kinetic model ($R^2 = 0.996$). Ramalingam and Subramania [70] in a research investigated the removal of nitrate from aqueous solutions using alumina nano-adsorbent and

Table 2
Results of goodness of fit of kinetic models on adsorption of nitrate ions by the studied adsorbents

Adsorption kinetics models	Pseudo-first-order kinetics				Pseudo-second-order kinetics			
Absorbent	K (min^{-1})	q_e (mg/g)	R^2	RMSE	K (g/mg·min)	q_e (mg/g)	R^2	RMSE
Eggshell	0.016	1.40	0.56	8.07	0.052	9.55	0.89	0.74
Rice husk	0.020	0.78	0.61	8.39	0.039	9.606	0.89	0.78
Straw	0.035	1.28	0.78	7.82	0.033	9.60	0.89	0.73
Oak leaf	0.029	4.78	0.97	4.85	0.015	9.93	0.99	0.15

Table 3
Results of the goodness of fit of isotherm models on adsorption of nitrate ions by the studied adsorbents

Adsorption isotherm models	Freundlich				Langmuir			
Absorbent	K (L/mg)	$1/n$	R^2	RMSE	q_m (mg/g)	b (L/mg)	R^2	RMSE
Eggshell	0.134	0.88	0.985	0.379	35.71	0.002	0.979	0.459
Rice husk	0.114	0.92	0.987	0.370	55.24	0.0016	0.984	0.404
Straw	0.105	0.93	0.988	0.366	76.92	0.0011	0.986	0.385
Oak leaf	0.120	0.91	0.990	0.373	48.30	0.0019	0.983	0.420

Table 4
Effect of changes in the concentration of inlet nitrate the column on effective parameters of adsorption by the studied sorbents

Sorbent flow	Flow rate (mL/min)	Inlet nitrate concentration (mg/L)	Total time (min)	Total nitrate entered into the column m_{total} (mg)	Total amount of adsorption q_{total} (mg)	Column adsorption capacity q_{eq} (mg/g)	Total removal (%)
	50	5	900	225	147.299	0.29	65.47
Eggshell	50	10	800	400	223.736	0.44	55.93
	50	30	680	1020	515.903	1.03	50.57
	50	5	500	125	57.757	0.49	46.20
Rice husk	50	10	400	200	89.745	0.76	44.87
	50	30	350	500	229.985	1.96	43.80
	50	5	400	100	45.999	0.57	45.99
Wheat straw	50	10	350	175	69.206	0.85	39.54
	50	30	300	450	157.912	1.95	35.09
	50	5	700	175	101.724	0.92	58.12
Oak leaf	50	10	620	310	159.028	1.45	51.29
	50	30	560	840	389.534	3.55	46.37

Pt anode and brass cathode electrochemical method. The results of this study showed that the maximum removal of nitrate ions by alumina nano-absorbent was achieved after 90 min at a concentration of 200 mg/L with a current concentration of 2 A/dm. Also, during the electrocatalytic reduction process, NO_3 ions absorbed on the platinum electrode was reduced to NO_2-nitrite ions and NO_2-ions to NO, N_2O and N_2 gas [70]. Also, Quang et al. [71] investigated the removal of nitrate from aqueous solution using ZrO_2 nanomaterials supported by biochar derived from watermelon rind. In this study, watermelon rind derived from biochar (WM) was produced through optimal pyrolysis at 500°C for 2 h, and then the adsorption capacity was improved by zirconium oxide nanoparticles (ZrO_2 NPs). In general, in this research, WM@ZrO_2 has been proposed as a promising, effective and environmentally friendly adsorbent for nitrate removal from aqueous solution.

5. Conclusion

This study aimed to evaluate nitrate removal from aqueous solutions using nanostructured adsorbents in continuous and discontinuous systems. In continuous tests, the optimal pH for nitrate ion adsorption by eggshell, rice husk, wheat straw and oak leaf nanostructured adsorbents was found to be 5. Equilibrium time for nitrate ion adsorption

Table 5
Results of the goodness of fit of continuous models on nitrate ion adsorption by the studied sorbents

Sorbent	Model	Nitrate concentration (mg/L)	K_{AB} (L/mg·min)	N_0 (mg/L)	R^2	RMSE
Eggshell	Adams–Bohart model	5	0.0014	493.9	0.74	3.22
		10	0.0007	798.4	0.67	8.83
		30	0.0002	2,253.3	0.82	11.48
			K_{Th} (L/g·min)	q_0 (mg/g)	R^2	RMSE
	Thomas model	5	0.0017	306.42	0.99	0.21
		10	0.0009	476.15	0.99	0.55
		30	0.0003	1,179.98	0.99	2.11
			K_{YN} (min^{-1})	τ (min)	R^2	RMSE
	Yoon–Nelson model	5	0.008	610.4	0.99	0.22
		10	0.009	454.08	0.98	0.47
		30	0.0101	345.9	0.98	1.31
Rice husk	Adams–Bohart model		K_{AB} (L/mg·min)	N_0 (mg/L)	R^2	RMSE
		5	0.003	259.009	0.43	8.37
		10	0.001	439.32	0.69	4.50
		30	0.0003	1,253.17	0.81	6.02
	Thomas model		K_{Th} (L/g·min)	q_0 (mg/g)	R^2	RMSE
		5	0.004	575.75	0.98	0.37
		10	0.001	853.29	0.98	0.57
		30	0.0005	2,295.10	0.99	2.09
	Yoon–Nelson model		K_{YN} (min^{-1})	τ(min)	R^2	RMSE
		5	0.027	220.8	0.97	0.37
		10	0.018	442.4	0.98	0.58
		30	0.014	182.3	0.99	2.22
Wheat straw	Adams–Bohart model		K_{AB} (L/mg·min)	N_0 (mg/L)	R^2	RMSE
		5	0.002	215.1	0.58	3.93
		10	0.001	393.6	0.69	3.56
		30	0.0003	1,670.6	0.76	13.02
	Thomas model		K_{Th} (L/g·min)	q_0 (mg/g)	R^2	RMSE
		5	0.004	698.78	0.98	0.43
		10	0.001	1,076.46	0.97	0.87
		30	0.0005	2,538.39	0.97	2.90
	Yoon–Nelson model		K_{YN} (min^{-1})	τ (min)	R^2	RMSE
		5	0.02	224.1	0.97	0.43
		10	0.018	172.53	0.97	0.88
		30	0.015	134.57	0.97	3.00
Oak leaf	Adams–Bohart model		K_{AB} (L/mg·min)	N_0 (mg/L)	R^2	RMSE
		5	0.0015	419.4	0.78	1.51
		10	0.0007	673.13	0.80	5.06
		30	0.0002	2,353.34	0/81	7.54
	Thomas model		K_{Th} (L/g·min)	q_0 (mg/g)	R^2	RMSE
		5	0.0025	913.05	0.99	0.13
		10	0.0011	1,520.60	0.99	0.32
		30	0.0004	3,663.07	0.99	1.03
	Yoon–Nelson model		K_{YN} (min^{-1})	τ (min)	R^2	RMSE
		5	0.012	406.8	0.99	0.16
		10	0.011	333.3	0.99	0.33
		30	0.014	236.7	0.97	2.14

by eggshell, rice husk, and wheat straw nanostructured adsorbents was 30 min and 120 min in oak leaf adsorbent. After these times, the adsorption efficiency approximately had a constant trend. According to the results of discontinuous tests, 0.5 g in eggshell, rice husk, and wheat straw nanostructure adsorbents, and 0.7 g in oak leaf adsorbent were determined as the optimal amount of adsorbent for nitrate adsorption. Also, the highest efficiency of removal of nitrate ions by nanostructured adsorbents of eggshell, rice husk, wheat straw and oak leaf occurred at a concentration of 5 mg/L. Investigations showed that the adsorption process obeyed the pseudo-second-order kinetic model and the Langmuir isotherm model. In general, the results of the continuous tests showed that the total amount of nitrate adsorbed by eggshell, rice husk, wheat straw and oak leaf nanostructure adsorbents increases with the increase of nitrate concentration entering the column. In terms of fitting of continuous adsorption models on experimental data by eggshell, rice husk, wheat straw and oak leaf adsorbents in nitrate adsorption using fixed bed column, Thomas model had a better fitting in adsorption column data than Adams–Bohart and Yoon–Nelson models. Based on the results of this research, eggshell, rice husk, wheat straw, and oak leaf adsorbents had high potential in removing nitrate ions.

References

[1] Y. Liu, P. Wang, B. Gojenko, J. Yu, L. Wei, D. Luo, T. Xiao, A review of water pollution arising from agriculture and mining activities in Central Asia: facts, causes and effects, Environ. Pollut., 291 (2021) 118209, doi: 10.1016/j.envpol.2021.118209.

[2] M.H. Ward, R.R. Jones, J.D. Brender, T.M. de Kok, P.J. Weyer, B.T. Nolan, C.M. Villanueva, S.G. van Breda, Drinking water nitrate and human health: an updated review, Int. J. Environ. Res. Public Health, 15 (2018) 1557, doi: 10.3390/ijerph15071557.

[3] M. Amini, R. Dehghan, Assessment of physical, chemical and microbial quality of drinking water of Jiroft City, J. Environ. Sci. Technol., 23 (2021) 47–58.

[4] T.A. Saleh, M. Mustaqeem, M. Khaled, Water treatment technologies in removing heavy metal ions from wastewater: a review, Environ. Nanotechnol. Monit. Manage., 17 (2022) 100617, doi: 10.1016/j.enmm.2021.100617.

[5] P. Mehrabinia, E. Ghanbari-Adivi, Examining nitrate surface adsorption method from polluted water using activated carbon of agricultural wastes, Model. Earth Syst. Environ., 8 (2022) 1553–1561.

[6] M. Bahrami, M.J. Amiri, Nitrate removal from contaminated waters using modified rice husk ash by hexadecyltrimethylammonium bromide surfactant, React. Kinet. Mech. Catal., 135 (2022) 459–478.

[7] R. Djeribi, O. Hamdaoui, Sorption of copper(II) from aqueous solutions by cedar sawdust and crushed brick, Desalination, 225 (2008) 95–112.

[8] E. Polat, M. Karaca, H. Demir, A.N. Onus, Use of natural zeolite (clinoptilolite) in agriculture, J. Fruit Ornam. Plant Res, 12 (2004) 183–189.

[9] H. Aydın, Y. Bulut, Ç. Yerlikaya, Removal of copper(II) from aqueous solution by adsorption onto low-cost adsorbents, J. Environ. Manage., 87 (2008) 37–45.

[10] N. Singh, G. Nagpal, S. Agrawal, Water purification by using adsorbents: a review, Environ. Technol. Innovation, 11 (2018) 187–240.

[11] S. Manikandan, R. Subbaiya, M. Saravanan, M. Ponraj, M. Selvam, A. Pugazhendhi, A critical review of advanced nanotechnology and hybrid membrane based water recycling, reuse, and wastewater treatment processes, Chemosphere, 289 (2022) 132867, doi: 10.1016/j.chemosphere.2021.132867.

[12] D.E. Egirani, N. Shehata, M.H. Khedr, A review of nano materials in agriculture and allied sectors: preparation, characterization, applications, opportunities, and challenges, Mater. Int., 2 (2020) 421–432.

[13] D. Jassby, T.Y. Cath, H. Buisson, The role of nanotechnology in industrial water treatment, Nat. Nanotechnol., 13 (2018) 670–672.

[14] V. Alimohammadi, M. Sedighi, E. Jabbari, Response surface modeling and optimization of nitrate removal from aqueous solutions using magnetic multi-walled carbon nanotubes, J. Environ. Chem. Eng., 4 (2016) 4525–4535.

[15] J.-Y. Huang, W.-R. Liu, Synthesis and characterizations of $CoCr_2O_4$/C composite using high energy ball-milling technique as novel anode materials for Li-ion batteries, J. Chin. Inst. Chem. Eng., 96 (2019) 205–213.

[16] K. Mukherjee, R. Gupta, G. Kumar, S. Kumari, S. Biswas, P. Padmanabhan, Synthesis of silver nanoparticles by *Bacillus clausii* and computational profiling of nitrate reductase enzyme involved in production, J. Genet. Eng. Biotechnol., 16 (2018) 527–536.

[17] P. Bahmani, A. Maleki, H. Daraei, M. Khamforoush, S.D. Athar, F. Gharibi, Fabrication and characterization of novel polyacrylonitrile/α-Fe_2O_3 ultrafiltration mixed-matrix membranes for nitrate removal from aqueous solutions, J. Mol. Liq., 271 (2018) 557–570.

[18] H.T. Banu, S. Meenakshi, One pot synthesis of chitosan grafted quaternized resin for the removal of nitrate and phosphate from aqueous solution, Int. J. Biol. Macromol., 104 (2017) 1517–1527.

[19] Z. Abousalman-Rezvani, P. Eskandari, H. Roghani-Mamaqani, M. Salami-Kalajahi, Synthesis of coumarin-containing multi-responsive CNC-grafted and free copolymers with application in nitrate ion removal from aqueous solutions, Carbohydr. Res., 225 (2019) 115247, doi: 10.1016/j.carbpol.2019.115247.

[20] M. Keshvardoostchokami, S. Babaei, F. Piri, A. Zamani, Nitrate removal from aqueous solutions by ZnO nanoparticles and chitosan-polystyrene–Zn nanocomposite: kinetic, isotherm, batch and fixed-bed studies, Int. J. Biol. Macromol., 101 (2017) 922–930.

[21] E. Derakhshani, A. Naghizadeh, A.R. Yari, M.J. Mohammadi, M. Kamranifar, M. Farhang, Association of toxicochemical and microbiological quality of bottled mineral water in Birjand city, Iran, Toxin Rev., 37 (2018) 138–143.

[22] S.K. Lagergren, About the theory of so-called adsorption of soluble substances, K. Sven. Vetenskapsakad. Handl., 24 (1898) 1–39.

[23] Y.-S. Ho, G. McKay, Pseudo-second order model for sorption processes, Process Biochem., 34 (1999) 451–465.

[24] M. Sayadi, M. Farasati, M.G. Mahmoodlu, F. Rostami Charati, Removal of nitrate, ammonium, and phosphate from water using Conocarpus and Paulownia plant biochar, Iran. J. Chem. Chem. Eng., 39 (2020) 205–222.

[25] I. Langmuir, The adsorption of gases on plane surfaces of glass, mica and platinum, J. Am. Chem. Soc., 40 (1918) 1361–1403.

[26] H. Freundlich, Over the adsorption in solution, J. Phys. Chem., 57 (1906) 1100–1107.

[27] E. Karamati-Niaragh, M.R.A. Moghaddam, M.M. Emamjomeh, E. Nazlabadi, Evaluation of direct and alternating current on nitrate removal using a continuous electrocoagulation process: economical and environmental approaches through RSM, J. Environ. Manage., 230 (2019) 245–254.

[28] Z. Aksu, F. Gönen, Biosorption of phenol by immobilized activated sludge in a continuous packed bed: prediction of breakthrough curves, Process Biochem., 39 (2004) 599–613.

[29] J.-L. Gong, Y.-L. Zhang, Y. Jiang, G.-M. Zeng, Z.-H. Cui, K. Liu, C.-H. Deng, Q.-Y. Niu, J.-H. Deng, S.-Y. Huan, Continuous adsorption of Pb(II) and methylene blue by engineered graphite oxide coated sand in fixed-bed column, Appl. Surf. Sci., 330 (2015) 148–157.

[30] A.P. Lim, A.Z. Aris, Continuous fixed-bed column study and adsorption modeling: removal of cadmium(II) and lead(II) ions in aqueous solution by dead calcareous skeletons, Biochem. Eng. J., 87 (2014) 50–61.
[31] R. Aravindhan, J.R. Rao, B.U. Nair, Preparation and characterization of activated carbon from marine macro-algal biomass, J. Hazard. Mater., 162 (2009) 688–694.
[32] D.C. Ko, J.F. Porter, G. McKay, Optimised correlations for the fixed-bed adsorption of metal ions on bone char, Chem. Eng. Sci., 55 (2000) 5819–5829.
[33] A. Ghosh, S. Chakrabarti, U.C. Ghosh, Fixed-bed column performance of Mn-incorporated iron(III) oxide nanoparticle agglomerates on As(III) removal from the spiked groundwater in lab bench scale, Chem. Eng. J., 248 (2014) 18–26.
[34] H.C. Thomas, Heterogeneous ion exchange in a flowing system, J. Am. Chem. Soc., 66 (1944) 1664–1666.
[35] R. Han, Y. Wang, X. Zhao, Y. Wang, F. Xie, J. Cheng, M. Tang, Adsorption of methylene blue by phoenix tree leaf powder in a fixed-bed column: experiments and prediction of breakthrough curves, Desalination, 245 (2009) 284–297.
[36] X. Ren, X. Zhang, L. Zhang, R. Han, Biosorption of methylene blue by natural and chemical modified wheat straw in fixed-bed column, Desal. Water Treat., 51 (2013) 4514–4523.
[37] Y.H. Yoon, J.H. Nelson, Application of gas adsorption kinetics I. A theoretical model for respirator cartridge service life, Am. Ind. Hyg. Assoc. J., 45 (1984) 509–516.
[38] G.K. Rajahmundry, C. Garlapati, P.S. Kumar, R.S. Alwi, D.-V.N. Vo, Statistical analysis of adsorption isotherm models and its appropriate selection, Chemosphere, 276 (2021) 130176, doi: 10.1016/j.chemosphere.2021.130176.
[39] E. Mohammadi, H. Daraei, R. Ghanbari, S.D. Athar, Y. Zandsalimi, A. Ziaee, A. Maleki, K. Yetilmezsoy, Synthesis of carboxylated chitosan modified with ferromagnetic nanoparticles for adsorptive removal of fluoride, nitrate, and phosphate anions from aqueous solutions, J. Mol. Liq., 273 (2019) 116–124.
[40] H. Qiao, L. Mei, G. Chen, H. Liu, C. Peng, F. Ke, R. Hou, X. Wan, H. Cai, Adsorption of nitrate and phosphate from aqueous solution using amine cross-linked tea wastes, Appl. Surf. Sci., 483 (2019) 114–122.
[41] A. Rahmani, H.Z. Mousavi, M. Fazli, Effect of nanostructure alumina on adsorption of heavy metals, Desalination, 253 (2010) 94–100.
[42] M. Tehrani, M. Safdari, M. Al-Haik, Nanocharacterization of creep behavior of multiwall carbon nanotubes/epoxy nanocomposite, Int. J. Plast., 27 (2011) 887–901.
[43] F.D. Belkada, O. Kitous, N. Drouiche, S. Aoudj, O. Bouchelaghem, N. Abdi, H. Grib, N. Mameri, Electrodialysis for fluoride and nitrate removal from synthesized photovoltaic industry wastewater, Sep. Purif. Technol., 204 (2018) 108–115.
[44] B. Mehdinejadiani, S.M. Amininasab, L. Manhooei, Enhanced adsorption of nitrate from water by modified wheat straw: equilibrium, kinetic and thermodynamic studies, Water Sci. Technol. Lib., 79 (2019) 302–313.
[45] P. Karthikeyan, S. Meenakshi, Enhanced removal of phosphate and nitrate ions by a novel ZnFe LDHs-activated carbon composite, Sustainable Mater. Technol., 25 (2020) e00154, doi: 10.1016/j.susmat.2020.e00154.
[46] Z. Kheshti, K.A. Ghajar, A. Altaee, M. Kheshti, High-gradient magnetic separator (HGMS) combined with adsorption for nitrate removal from aqueous solution, Sep. Purif. Technol., 212 (2019) 650–659.
[47] M. Muthu, D. Ramachandran, N. Hasan, M. Jeevanandam, J. Gopal, S. Chun, Unprecedented nitrate adsorption efficiency of carbon-silicon nano composites prepared from bamboo leaf, Mater. Chem. Phys., 189 (2017) 12–21.
[48] A. Battas, A.E. Gaidoumi, A. Ksakas, A. Kherbeche, Adsorption study for the removal of nitrate from water using local clay, Sci. World J., 2019 (2019) 9529618, doi: 10.1155/2019/9529618.
[49] A. Azari, M. Yeganeh, M. Gholami, M. Salari, The superior adsorption capacity of 2,4-dinitrophenol under ultrasound-assisted magnetic adsorption system: modeling and process optimization by central composite design, J. Hazard. Mater., 418 (2021) 126348, doi: 10.1016/j.jhazmat.2021.126348.
[50] P. Karthikeyan, H.A.T. Banu, S. Meenakshi, Removal of phosphate and nitrate ions from aqueous solution using La^{3+} incorporated chitosan biopolymeric matrix membrane, Int. J. Biol. Macromol., 124 (2019) 492–504.
[51] R. Gouran-Orimi, B. Mirzayi, A. Nematollahzadeh, A. Tardast, Competitive adsorption of nitrate in fixed-bed column packed with bio-inspired polydopamine coated zeolite, J. Environ. Chem. Eng., 6 (2018) 2232–2240.
[52] X. Xu, B. Gao, X. Tan, X. Zhang, Q. Yue, Y. Wang, Q. Li, Nitrate adsorption by stratified wheat straw resin in lab-scale columns, Chem. Eng. J., 226 (2013) 1–6.
[53] J. Goel, K. Kadirvelu, C. Rajagopal, V.K. Garg, Removal of lead(II) by adsorption using treated granular activated carbon: batch and column studies, J. Hazard. Mater., 125 (2005) 211–220.
[54] Y.K. Recepoğlu, N. Kabay, I.Y. Ipek, M. Arda, M. Yüksel, K. Yoshizuka, S. Nishihama, Packed bed column dynamic study for boron removal from geothermal brine by a chelating fiber and breakthrough curve analysis by using mathematical models, Desalination, 437 (2018) 1–6.
[55] A. Olgun, N. Atar, S. Wang, Batch and column studies of phosphate and nitrate adsorption on waste solids containing boron impurity, Chem. Eng. J., 222 (2013) 108–119.
[56] P. Karthikeyan, S. Vigneshwaran, S. Meenakshi, Removal of phosphate and nitrate ions from water by amine crosslinked magnetic banana bract activated carbon and its physicochemical performance, Environ. Nanotechnol. Monit. Manage., 13 (2020) 100294, doi: 10.1016/j.enmm.2020.100294.
[57] W. Zhang, J. Shen, H. Zhang, C. Zheng, R. Wei, Y. Gao, L. Yang, Efficient nitrate removal by *Pseudomonas mendocina* GL6 immobilized on biochar, Bioresour. Technol., 320 (2021) 124324, doi: 10.1016/j.biortech.2020.124324.
[58] S.Y. Hashemi, M. Yegane Badi, H. Pasalari, A. Azari, H. Arfaeinia, A. Kiani, Degradation of ceftriaxone from aquatic solution using a heterogeneous and reusable O_3/UV/Fe_3O_4@TiO_2 systems: operational factors, kinetics and mineralisation, Int. J. Environ. Anal. Chem., 102 (2022) 6904–6920.
[59] M. Farasati, M. Seyedian, S. Boroomandnasab, N. Jaafarzadeh, H. Moazed, H. Ghamarnia, Batch and column studies on the evaluation of micrometer and nanometer *Phragmites australis* for nitrate removal, Desal. Water Treat., 51 (2013) 5863–5872.
[60] I.A. Kumar, C. Jeyaprabha, N. Viswanathan, Effect of polyvalent metal ions encrusted biopolymeric hybrid beads on nitrate adsorption, J. Environ. Chem. Eng., 8 (2020) 103894, doi: 10.1016/j.jece.2020.103894.
[61] R.A. Rao, F. Rehman, Adsorption studies on fruits of gular (*Ficus glomerata*): removal of Cr(VI) from synthetic wastewater, J. Hazard. Mater., 181 (2010) 405–412.
[62] R. Katal, M.S. Baei, H.T. Rahmati, H. Esfandian, Kinetic, isotherm and thermodynamic study of nitrate adsorption from aqueous solution using modified rice husk, J. Ind. Eng. Chem., 18 (2012) 295–302.
[63] S. Rahdar, K. Pal, L. Mohammadi, A. Rahdar, Y. Goharniya, S. Samani, G.Z. Kyzas, Response surface methodology for the removal of nitrate ions by adsorption onto copper oxide nanoparticles, J. Mol. Struct., 1231 (2021) 129686, doi: 10.1016/j.molstruc.2020.129686.
[64] I. Fernandez-Olmo, J. Fernandez, A. Irabien, Purification of dilute hydrofluoric acid by commercial ion exchange resins, Sep. Purif. Technol., 56 (2007) 118–125.
[65] T. Wang, J. Lin, Z. Chen, M. Megharaj, R. Naidu, Green synthesized iron nanoparticles by green tea and eucalyptus leaf extracts used for removal of nitrate in aqueous solution, J. Cleaner Prod., 83 (2014) 413–419.
[66] P.N. Fotsing, N. Bouazizi, E.D. Woumfo, N. Mofaddel, F. Le Derf, J. Vieillard, Investigation of chromate and nitrate removal by adsorption at the surface of an amine-modified cocoa shell adsorbent, J. Environ. Chem. Eng., 9 (2021) 104618, doi: 10.1016/j.jece.2020.104618.
[67] M. Bahrami, M.J. Amiri, B. Beigzadeh, Adsorption of 2,4-dichlorophenoxyacetic acid using rice husk biochar, granular activated carbon, and multi-walled carbon nanotubes

in a fixed bed column system, Water Sci. Technol., 78 (2018) 1812–1821.
[68] A. Azari, A.-A. Babaie, R. Rezaei-Kalantary, A. Esrafili, M. Moazzen, B. Kakavandi, Nitrate removal from aqueous solution by carbon nanotubes magnetized with nano zero-valent iron, J. Mazandaran Univ. Med. Sci., 23 (2014) 15–27.
[69] A. Takdastan, S. Pourfadakari, S. Jorfi, Ultrasonically induced adsorption of nitrate from aqueous solution using Fe_3O_4@ activated carbon nanocomposite, Desal. Water Treat., 123 (2018) 230–239.
[70] S. Ramalingam, A. Subramania, Effective removal of nitrates from the drinking water by chemical and electrochemical methods, Eng. Sci., 15 (2021) 80–88.
[71] H.H.P. Quang, K.T. Phan, P.D.L. Ta, N.T. Dinh, T.S. Alomar, N. AlMasoud, C.-W. Huang, A. Chauhan, V.-H. Nguyen, Nitrate removal from aqueous solution using watermelon rind derived biochar-supported ZrO_2 nanomaterial: synthesis, characterization, and mechanism, Arabian J. Chem., 15 (2022) 104106, doi: 10.1016/j.arabjc.2022.104106.